Melting Behavior, Isothermal and Nonisothermal Crystallization Kinetics of EPPE/mLLDPE Blends

Jianglei Qin, Kuilin Deng, Zhiting Li

Department of Polymer Science, College of Chemistry and Environmental Science, Hebei University, Baoding 071002, China

Received 25 October 2007; accepted 9 January 2008
DOI 10.1002/app.27967
Published online 6 March 2008 in Wiley InterScience (www.interscience.wiley.com).

ABSTRACT: Melting behavior and crystallization kinetics of easy processing polyethylene (EPPE) and the blends of EPPE/mLLDPE were studied using differential scanning calorimetry at various crystallization temperature and cooling rates. The Avrami analysis was employed to describe the isothermal and nonisothermal crystallization process of pure polymers and their blends, and a method developed by Mo was applied for comparison. Kinetic parameters such as the Avrami exponent (n), the kinetic crystallization rate constant (k and k_c), the peak temperatures (T_p), and the half-time of crystallization ($t_{1/2}$), etc. were determined. The appearance of double melting peaks and the double crystallization peaks of the polymers showed that the main chain and the branches crystallize seperately, but the main chains of two polymers can crystallize together and mLLDPE act as nuclei while EPPE crystallizes. © 2008 Wiley Periodicals, Inc. J Appl Polym Sci 108: 3601–3609, 2008

Key words: easy processing polyethylene; metallocene-catalyzed low density polyethylene; blends; crystallization kinetics

INTRODUCTION

Polyethylene (PE)[1] is currently the most widely used commercial polymer in the world. Because of its specific properties such as high chemical resistance and mechanical property, easy processibility, low specific density and cost, the industrial PE market is still growing. And new grades of PE with better property are eagerly awaited.

Easy processing polyethylene (EPPE) is a new kind of PE material, it is the copolymer of ethylene and long-chain α-olefins with new metallocene catalyzer. Because of the tactic long branches in the EPPE molecules, its rheological behavior is similar to that of LDPE. At the same time, high tacticity of branches keep good mechanical property like LLDPE, then combines good mechanical property and good processability. As a result, its properties are superior to those of conventional PE and mPE, and it has a wide variety of new applications. While blending with other PE materials, compared to LDPE, EPPE can endow with good processability and good surface property without loss of mechanical properties.

Investigations of polymer crystallization kinetics[2,3] are significant both theoretically and practically. Most frequently, the investigations are conducted under isothermal conditions because the crystallization parameters can indicate the nucleation and growing mechanism of the crystal. But investigations of nonisothermal crystallization behavior can give to a guide for processing and application. As a result, a study on the isothermal and nonisothermal crystallization kinetics of EPPE/mLLDPE blends is more meaningful. However, studies on EPPE and its blends have never been reported yet.

In this article, the Avrami analysis and/or modified by Jeziorny and a method developed by Mo were employed to describe the crystallization kinetics of EPPE/mLLDPE blends. As a result, the crystallization behavior of EPPE/mLLDPE blends obeys the Avrami equation and Mo method as well.

EXPERIMENTAL

Materials

EPPE [GT140, melting flow rate (190°C/2.16 kg) = 0.9 g/10 min] was a production of Sumitomo Chemical (Tokyo, Japan); mLLDPE [ECD342, melting flow rate (190°C/2.16 kg) = 1.0 g/10 min] was obtained from Exxon Mobil Petrochemical (Houston, TX).

Preparation of EPPE/mLLDPE blends

The blending processes were carried out in a XSS-300 torque rheometer with a LH60 blender (Kechuang Machinery, China). The temperatures of the blender were set at 140°C. The weight ratios of EPPE to mLLDPE are 100/0; 90/10; 80/20; 50/50; 20/80; 0/100, respectively.

Correspondence to: J. Qin (thunder20@163.com).

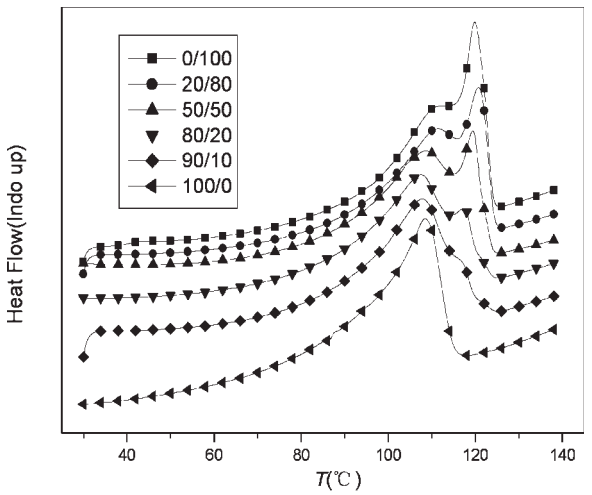

Figure 1 DSC melting curves of EPPE/mLLDPE blends at a heating rate of 10°C/min.

Thermal measurements

Thermal measurements were carried out on a Diamond DSC-7 differential scanning calorimeter (DSC, Perkin–Elmer, USA) with a sample weight of about 8.5 mg, all the operations were carried out under a nitrogen environment. The temperature and melting enthalpy were calibrated with standard indium.

For melting and crystallization behaviors, samples were heated from room temperature to 140°C at a heating rate of 10°C/min, and the temperature was held at 140°C for 1 min to erase thermal history. And then the samples were cooled to 30°C at a cooling rate of 10°C/min.

For nonisothermal crystallization, samples were heated to 140°C and held for 1 min, then cooled down to 30°C at various constant cooling rates: 2.5, 5, 10,15, and 20°C/min. As for isothermal crystallization kinetics, samples were cooled from 140°C down to the required crystallization temperature with a cooling rate of 150°C/min and hold for 30 min to record the heat flow. The half-time of crystallization ($t_{1/2}$) is defined as the time taken for 50% crystallinity.

RESULTS AND DISCUSSION

Melting and crystallization behavior of EPPE/mLLDPE blends

Figure 1 shows the heat flow of pure polymers and their blends at a heating rate of 10°C/min. From Figure 1, we can see that the pure mLLDPE shows two peaks in melting process and its melting temperature is obviously higher than that of EPPE. This is because the branches in EPPE are obviously longer than that in mLLDPE, the crystallization ability of EPPE is accordingly lower. The two melting peaks of mLLDPE are 112.4 and 119.8°C separately, and the melting peak of EPPE is 108.4°C. At the same time, most of the blend samples show two melting peaks, when the mLLDPE content is lower than 50/50, the melting temperature of EPPE decreases gradually with increasing mLLDPE content, showing the decrease of the crystal stability. However when the content of mLLDPE is higher than 50/50, the melting peak of EPPE approaches the lower peak of mLLDPE showing interaction of two components. All the melting and crystallizing temperatures of the blends are listed in Table I.

TABLE I
Melting Temperature (T_m) and Crystallization Temperature (T_c) of EPPE/mLLDPE Blends (°C)

EPPE/mLLDPE	100/0	90/10	80/20	50/50	20/80	0/100
T_{m1}	108.4	107.7	107.5	108.5	111.5	112.3
T_{m2}	–	–	117.2	119.4	120.7	119.8
T_{c1}	98.4	101.1	103.3	106.2	106.5	106.2
T_{c2}	60.5	61.8	62.6	66.0	68.2	69.8

The crystallization behavior were also performed by DSC at a cooling rate of 10°C/min. Figure 2 shows the crystallization exotherms of EPPE/mLLDPE blends when compared with pure polymers, respectively. All DSC traces show two crystallization peaks including those of pure polymers, indicating that these systems of blends exist as two crystallizable components. The two exotherm peaks of mLLDPE are 106.2 and 69.8°C separately, and the 69.8°C should be the crystallization temperature of branches. The two exothermal peaks of EPPE are 98.4 and 60.5°C, and 60.5°C is the crystallization temperature of long branches. The crystallization temperature of mLLDPE is much higher than EPPE and

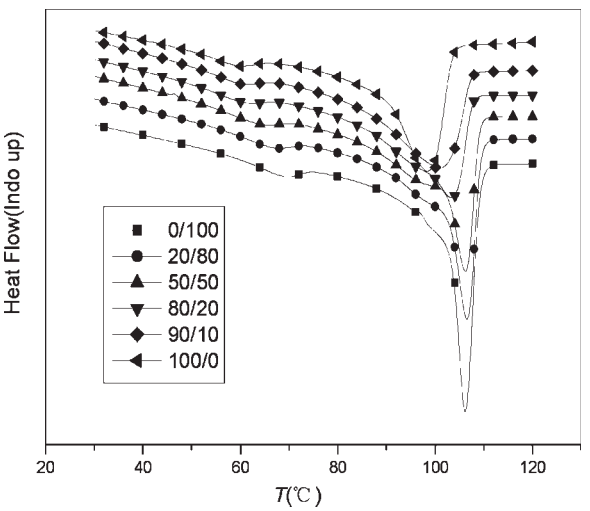

Figure 2 DSC nonisothermal crystallization curves of EPPE/mLLDPE blends at a cooling rate of 10°C/min.

the heat flow peak is much sharp, showing higher crystallization ability of mLLDPE main chains than that of EPPE. This is because of the existence of long and tactic branches in EPPE molecules, while the branches in mLLDPE molecules are much short.

The theories of crystallization kinetics

Up to date, several analytical methods have been developed to describe the crystallization kinetic of polymers, as follows: (i) Avrami analysis,[4–9] (ii) Ozawa analysis,[10,11] (iii) Ziabicki analysis,[12,13] and (iv) others[14–17] such as the Mo analysis. In this article, the Avrami analysis was used to describe the crystallization kinetics of EPPE/mLLDPE blends and the Mo analysis was taken as a contrastive study.

The Avrami equation[4-6,9,18,19] has been widely used to describe isothermal crystallization kinetics of polymers as follows:

$$1 - X_t = \exp(-kt^n) \tag{1}$$

where X_t is the relative crystallinity, k is the growth rate constant, and n is the Avrami exponent. Here, the value of Avrami exponent n depends on the nucleation mechanism and growth dimension; the parameter k is a function of the nucleation and the growth rate. The relative crystallinity X_t, as a function of crystallization time is defined as follows:

$$X_t = \frac{\int_0^t (dH/dt)dt}{\int_0^\infty (dH/dt)dt} \tag{2}$$

where dH/dt is the rate of heat evolution; t_0 and t_∞ were the time at which crystallization starts and ends, respectively.

Rewritten eq. (1) in a double logarithm form:

$$\log[-\ln(1 - X_t)] = \log(k) + n\log(t) \tag{3}$$

The Avrami equation can be modified to describe nonisothermal crystallization.[7,8,20,21] For nonisothermal crystallization at a chosen cooling rate, the relative crystallinity X_t is a function of crystallization temperature. That is, eq. (2) can be rewritten as follows:

$$X_t = \frac{\int_0^T (dH/dT)dT}{\int_0^\infty (dH/dT)dT} \tag{4}$$

where T is the crystallization temperature, T_0 and T_∞ represents the onset and end temperature of crystallization, respectively.

The crystallization temperature can be converted to crystallization time t using an equation.[13,21]

$$t = \frac{T_0 - T}{D} \tag{5}$$

where D is the cooling rate.

The half-time of crystallization ($t_{1/2}$)[22] is the time required for 50% crystallization. The lower the value of $t_{1/2}$, the higher is the crystallization rate.

Where T is the temperature of crystallization time t, and D is the cooling rate. From (3) and (5), we have eq. (6):

$$\log[-\ln(1 - X_t)] = \log(k') + n\log\left(\frac{T_0 - T}{D}\right) \tag{6}$$

where n is the Avrami exponent, which depends on the type of nucleation and growth dimension, and the parameter k is a composite rate constant that involves both nucleation and growth rate parameters. The Avrami exponent (n) and crystallization rate constant (k) can be obtained from the slope and intercept of the line in the plot of $\log[-\ln(1 - X_t)]$ versus $\log(\frac{T_0-T}{D})$. Considering the effect of the cooling rate, k is corrected by the cooling rate as follows[21]:

$$\log(k_c) = \frac{\log(k')}{D} \tag{7}$$

where k_c is the kinetic crystallization rate constant.

Ozawa[10,11] extended the Avrami equation to the nonisothermal condition. Assuming that the nonisothermal crystallization process may be composed of infinitesimally small isothermal crystallization steps, the following equation was derived:

$$1 - X_t = \exp[-K(T)/D^m] \tag{8}$$

or

$$\log[-\ln(1 - X_t)] = \log K(T) - m\log D \tag{9}$$

where $K(T)$ is the function of cooling rate and m is the Ozawa exponent, which is dependent on the dimension of the crystal growth.

A method developed by Mo[14] was also employed to describe the nonisothermal crystallization for comparison. For the process, physical variables relating to the process are the relative degree of crystallinity X_t, cooling rate D, and crystallization temperature T. Both the Ozawa and Avrami equations can relate these variables as follows:

$$\log Z_t + n\log t = \log K(T) - m\log D \tag{10}$$

And by rearrangement,

$$\log D = \log F(T) - a\log t \tag{11}$$

where $F(T) = [K(T)/Z_t]^{1/m}$ refers to the cooling rate value, which must be chosen within unit crystalliza-

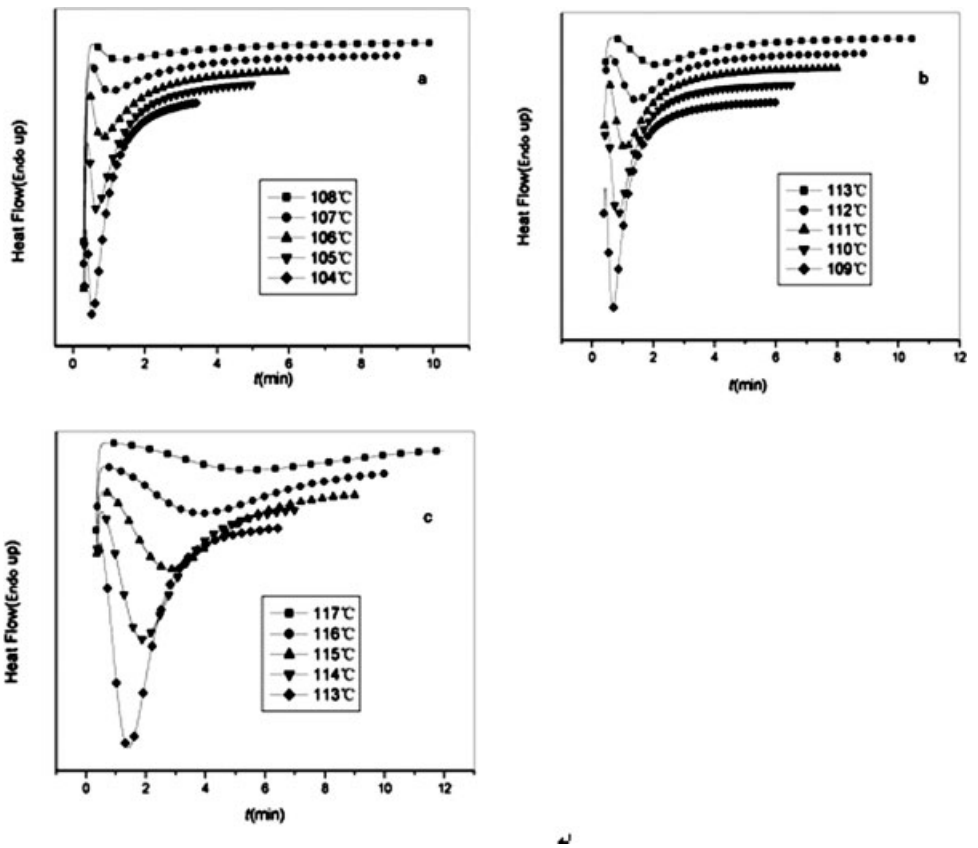

Figure 3 DSC isothermal crystallization curves of EPPE/mLLDPE blends at various crystallization temperatures [(a) 100/0; (b) 80/20; (c) 0/100].

tion time when the measured system amounts to a certain relative degree of crystallinity, which reflects the difficulty of its crystallization process, then the $F(T)$ value has a definite physical and practical meaning; a is the ratio of the Avrami exponent n to the Ozawa exponent m ($a = n/m$). According to eq. (11), $F(T)$ and a can be determined from the slope and intercept of logarithm plot of cooling rate versus time at different relative crystallinity.

The degree of crystallinity (X_c)[23] is defined as follows:

$$X_c = \frac{\Delta H_f}{\Delta H_f^0} \tag{12}$$

where ΔH_f and ΔH_f^0 are the melting enthalpies of PE sample and 100% crystallization PE, respectively, and $\Delta H_f^0 = 279$ J/g. ΔH_f is acquired by the integral area of a DSC heating curve.

Isothermal crystallization kinetics

Figure 3 shows the DSC traces for EPPE/mLLDPE blend that had been isothermally crystallized at different temperatures. It is obvious that the crystallization temperatures of pure polymers and blends are different; the crystallization temperature range of EPPE is lower than that of mLLDPE and the blends, similar to the result of crystallization behavior. Figure 4 shows the relative crystallinity of EPPE/mLLDPE (80/20) blends at various crystallization temperatures. All the curves in Figure 4 show a sig-

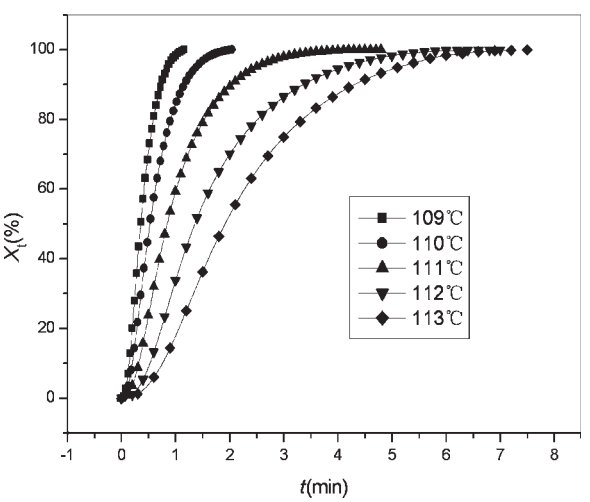

Figure 4 Plot of relative crystallinity X_t versus crystallization time t for EPPE/mLLDPE (80/20) blends at various crystallization temperatures.

TABLE II
Isothermal Crystallization Parameters of EPPE/mLLDPE Blends at Different Crystallization Temperatures

Sample (EPPE/mLLDPE)	T (°C)	N	log k	$t_{1/2}$ (min)	E_a (kJ/mol)
100/0	104	1.74	0.844	0.261	−566.7
	105	1.62	0.465	0.408	
	106	1.49	0.083	0.680	
	107	1.36	−0.245	1.14	
	108	1.41	−0.438	1.56	
	109	2.04	0.767	0.356	
	110	1.92	0.388	0.524	
80/20	111	1.90	−0.008	0.836	−528.5
	112	1.94	−0.402	1.36	
	113	2.00	−0.709	1.91	
	113	2.12	−0.333	1.18	
	114	2.03	−0.671	1.74	
0/100	115	2.14	−1.10	2.71	−464.2
	116	2.15	−1.42	3.80	
	117	2.36	−1.88	5.32	

moidal shape. The plot of X_t versus t shifts to the right with the increase in crystallization temperature, showing the decrease of crystallization rate, indicating the crystallization is enhanced as temperature decreases, this is because of the strong temperature dependence of the nucleation and the growth parameters.[24] The crystallization half-time $t_{1/2}$ can be calculated directly from the relative crystallinity versus time plot, see Table II.

Then, the Avrami parameters can be estimated from the slope and intercept of $\log[-\ln(1-X_t)]$ versus $\log t$ according to eq. (3). Figure 5 shows the plot of $\log[-\ln(1-X_t)]$ versus $\log t$ for isothermal crystallization of EPPE/mLLDPE (80/20) blends. Each curve shows good linear relationship indicating that the Avrami equation can properly describe the isothermal crystallization behavior of these samples. All the lines in Figure 5 are straight and almost paralleled to each other, shifting to less time with decreasing temperature. The Avrami parameters calculated from the plot of $\log[-\ln(1-X_t)]$ versus $\log t$ are listed in Table II. And there is an obvious secondary crystallization that existed in isothermal crystallization process.

The n values of EPPE increase and then decrease with increasing of crystallization temperature within 1.36–1.72, and that of the mLLDPE increase within the range of 2.03–2.36, while the n values of the blends are between those of two pure polymers. The increasing crystallization temperature of the blends than EPPE show that the mLLDPE act as nucleation agent while EPPE crystallizes. The low n values of EPPE show the low crystallization ability of it, because of the low crystallization ability of the long branches. At the same time, the values of Avrami parameters show the nucleation mechanism of both EPPE and mLLDPE, and their blends are heterogeneous, and the increasing of Avrami exponents means more perfection of the spherulites.

However, the crystallization rate is dependent on the blend composition and temperature. On one hand, for the pure EPPE, the crystallization rate constant (k) decreases with increasing temperature, and the crystallization half-time ($t_{1/2}$) increases (see Table II). Similar trends in both the k and $t_{1/2}$ are observed for the EPPE/mLLDPE (80/20) and mLLDPE. At the required temperature range, the k value of the blends and mLLDPE are obviously lower than that of EPPE. This is because of the required crystallization temperature of mLLDPE is obviously higher than that of EPPE, but from the intersectant temperature we can see the crystallization rate of mLLDPE is obviously higher than that of EPPE. However, because of the difference of crystallization tempera-

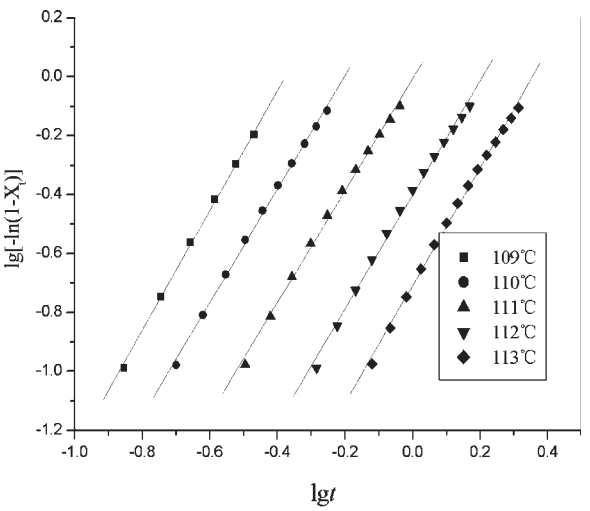

Figure 5 Avrami plot of EPPE/mLLDPE (80/20) blends at various crystallization temperatures.

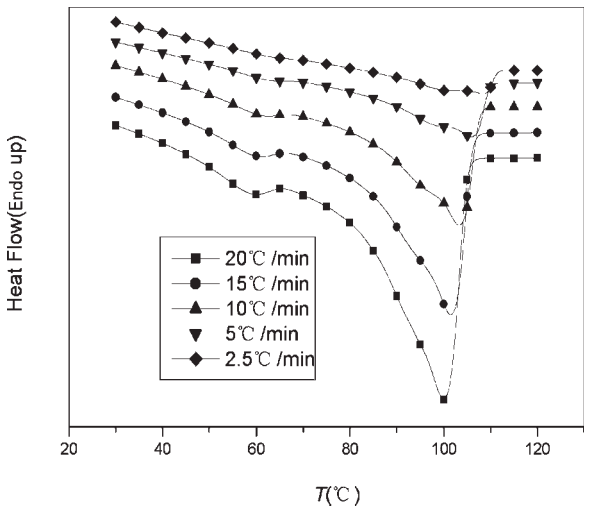

Figure 6 DSC nonisothermal crystallization curves for EPPE/mLLDPE (80/20) blends at various cooling rates.

ture ranges, the crystallization rate at given temperature cannot be compared.

Nonisothermal crystallization kinetic of EPPE/mLLDPE blends

As an example, Figure 6 shows the typical crystallization exotherms for EPPE/mLLDPE (80/20) at various cooling rates. The heat flow curve shifts to lower temperature region as the cooling rate increases. The lower cooling rate provides more fluidity and diffusivity for the molecules because of the relative lower viscosity and more time to crystallize, thus inducing higher crystallinity and more perfect crystallization at lower cooling rates, as shown in Table III. The crystallinity of EPPE increases gradually with decreasing of cooling rate. And when the cooling rate is low, the main chains and the branches crystallize separately; while the cooling rate is high, main chains and the branches crystallize together. The curves can be transformed to the plot of X_t versus t using eqs. (4) and (5), as shown in Figure 7. The sigmoidal shape of the curves suggests the modified Avrami analysis is applicable for nonisothermal crystallization of EPPE/mLLDPE blends. Meanwhile, the crystallization half-time $t_{1/2}$ can be calculated directly from the relative crystallinity versus time plot,[9,25] as shown in Table III.

Figure 8 shows the Avrami plot of $\log[-\ln(1-X_t)]$ versus $\log t$ for nonisothermal crystallization of EPPE/mLLDPE blends at various cooling rates. All the lines in Figure 8 are also straight and almost paralleled in first stages, implying that the nucleation mechanism and crystal growth geometries are similar, although the cooling rates are different. The Avrami parameters can be estimated from the plot of $\log[-\ln(1-X_t)]$ versus $\log t$, and the values are listed in Table III. Regardless of the cooling rates, the Avrami exponent n for the pure EPPE is in the range of 2.94–3.40, the Avrami exponents for the EPPE/mLLDPE (80/20) blends are in the range of 1.64–1.72, and that of pure mLLDPE are in the range of 3.35–6.12. The Avrami exponents of mLLDPE are higher than that of EPPE and the blends, because of its short and tactic branches. The Avrami exponents of the EPPE/mLLDPE (80/20) blends are the lowest because the mLLDPE crystallize first, and at that temperature the EPPE can hardly crystallize and cannot enter the spherulites, and then the spherulites are not perfect. But the Avrami exponents deduced from nonisothermal crystallization are not accurate because the temperatures of nonisothermal crystallization are changing continuously, and the crystallization rate constant k_c for nonisothermal crystallization should be corrected as follows[21]: $\log k_c = \log k'/D$.

As a result, the crystallization rate (k') increased with the cooling rate, whereas the crystallization

TABLE III
Nonisothermal Crystallization Parameters of EPPE/mLLDPE Blends at Different Cooling Rates

Sample (EPPE/mLLDPE)	D (°C/min)	n	$\log k_c$	$T_{1/2}$ (min)	T_p (°C)	ΔH (J/g)	Crystallinity (%)
100/0	2.5	2.95	−0.74	4.04	101.2	60.2	21.6
	5.0	3.19	−0.198	2.08	100.0	68.4	24.5
	10	3.33	0.004	1.03	98.5	71.7	25.7
	15	3.40	0.031	0.830	97.1	88.8	31.8
	20	3.39	0.042	0.634	95.9	90.5	32.4
	2.5	1.71	−0.516	4.58	108.4	62.9	22.6
	5.0	1.74	−0.172	2.56	105.9	77.4	27.7
80/20	10	1.64	−0.033	1.30	103.3	85.8	30.8
	15	1.70	−0.0067	0.943	101.4	93.0	33.3
	20	1.72	0.004	0.745	100.0	96.8	34.7
	2.5	3.35	−0.56	2.75	110.6	97.1	34.8
	5.0	5.36	−0.296	2.28	108.4	98.3	35.2
0/100	10	6.12	0.0016	1.16	106.1	99.5	35.7
	15	5.76	0.063	0.782	104.6	102.3	36.7
	20	3.96	0.069	0.511	103.4	104.8	37.6

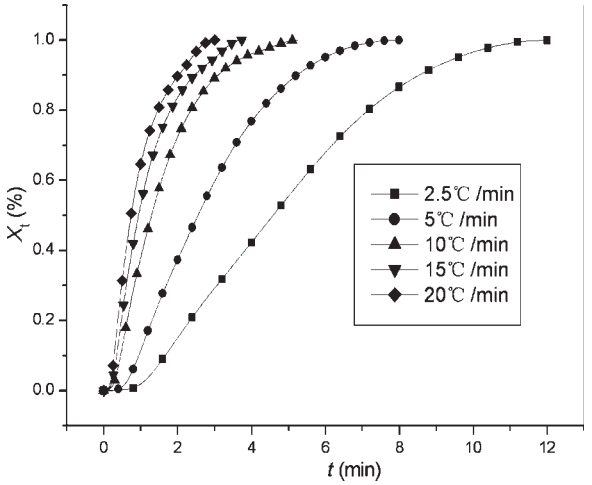

Figure 7 Plot of relative crystallinity X_t versus crystallization time t for EPPE/mLLDPE (80/20) blends at various cooling rates.

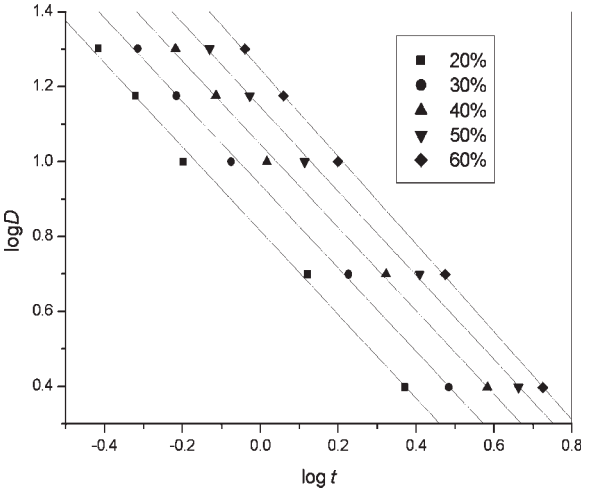

Figure 9 Mo plot for EPPE/mLLDPE (80/20) blends at different relative crystallinity.

half-time ($t_{1/2}$) decreased (see Table III). The crystallization rate of the blends is the lowest and the $t_{1/2}$ is the highest, because the mLLDPE crystallize first and act as nuclei for EPPE, but the EPPE cannot crystallize completely until the supercooling is high enough. The effects of mLLDPE on EPPE crystallization are the same in isothermal and nonisothermal crystallization kinetics. Whether at high temperatures (isothermal processes) or at lower temperatures (nonisothermal processes), the mLLDPE acts as nuclei for EPPE crystallization and increases the crystallization temperature of EPPE.

The Mo method is employed in this system for comparison. According to eq. (11), $F(T)$ and a of EPPE/mLLDPE blends can be determined from the slope and intercept of logarithm plot of cooling rate versus time at different relative crystallinity (X_t)of 20, 30,40, 50, and 60%, respectively. Figure 9 presents the result of EPPE/mLLDPE (80/20) blends according to the Mo method. Good fitness of the lines shows that the Mo method is successful for describing the nonisothermal crystallization process of EPPE/mLLDPE blends. The values of $F(T)$ and a of all the samples are listed in Table IV. The $F(T)$ values increase with the relative crystallinity for the same blend. However, at the same relative crystallinity, the values of $F(T)$ of EPPE are lower than that of EPPE/mLLDPE blends, implying the faster crystallization of EPPE than that of EPPE/mLLDPE blends. This conclusion is well consistent with the results obtained from modified Avrami analysis. The reason for this conclusion is because a large proportion of mLLDPE crystallization are owed to the crystallization of branches, and then the overall crystallization rate decrease; at the same time, the crystallization of

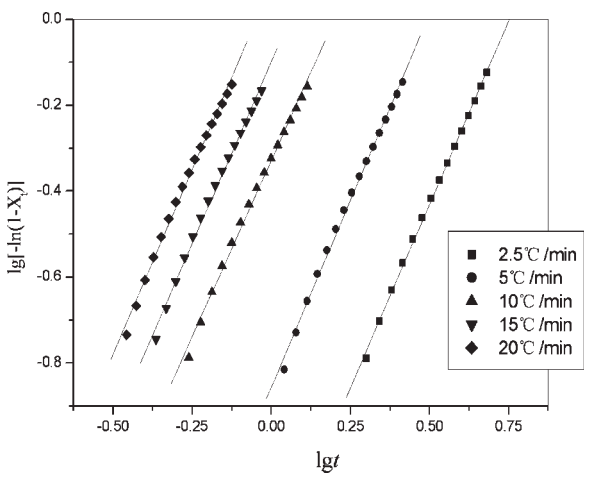

Figure 8 Avrami plot for EPPE/mLLDPE (80/20) blends at various cooling rates.

TABLE IV
Nonisothermal Crystallization Parameters of EPPE/mLLDPE Blends at Different Relative Crystallinity Based on Mo Method

Sample (EPPE/mLLDPE)	X_t (%)	ln $F(T)$	a	E_a (kJ/mol)
100/0	20	0.819	1.07	−384.7
	30	0.907	1.08	
	40	0.985	1.09	
	50	1.065	1.12	
	60	1.159	1.17	
80/20	20	0.816	1.12	−315.2
	30	0.939	1.11	
	40	1.046	1.05	
	50	1.146	1.12	
	60	1.247	1.17	
0/100	20	0.864	0.91	−355.9
	30	0.918	0.99	
	40	0.965	0.96	
	50	1.047	0.96	
	60	1.149	0.97	

EPPE branches are less important because of the low crystallization ability of the long branches of EPPE. The values of a for all the samples are around 1(0.91–1.17), showing consistency of Avrami exponents and Ozawa exponents.

The effect of mLLDPE on crystallization of EPPE are the same in isothermal and nonisothermal crystallization kinetics. The mLLDPE acts as nuclei and increased the crystallization temperature of EPPE.

Activation energy for crystallization

The activation energy for isothermal crystallization can be approximately described by the Arrhenius equation.[6,26,27]

$$k^{1/n} = k_0 \exp\left(-\frac{E_a}{RT_c}\right) \tag{13}$$

where R is the universal gas constant.

The slope of the Arrhenius plot of $(1/n)\ln k$ versus $1/T_c$ determines E_a/R, as shown in Figure 10. The value of the activation energy is found to be −566.7 kJ/mol for pure EPPE melt crystallization, −528.5 and −464.2 kJ/mol for EPPE/mLLDPE (80/20) and pure mLLDPE separately (Table II).

For nonisothermal crystallization, the crystallization activation energy E_a can be estimated from the variation of crystallization peak temperature T_p with cooling rate D by the Kissinger approach.[28]

$$\frac{d[\ln(D/T_p^2)]}{d(1/T_p)} = -\frac{E_a}{R} \tag{14}$$

where R is the universal gas constant.

The Kissinger plot, that is the plot of $\ln(D/T_p{}^2)$ versus $1/T_p$ for PP/mLLDPE blends, is shown in Figure 11. The E_a is estimated to be −384.7 kJ/mol for pure PP, −315.2 kJ/mol for the PP/(20%) mLLDPE blends, and −355.9 kJ/mol for PP/(40%) mLLDPE blends (see Table IV).

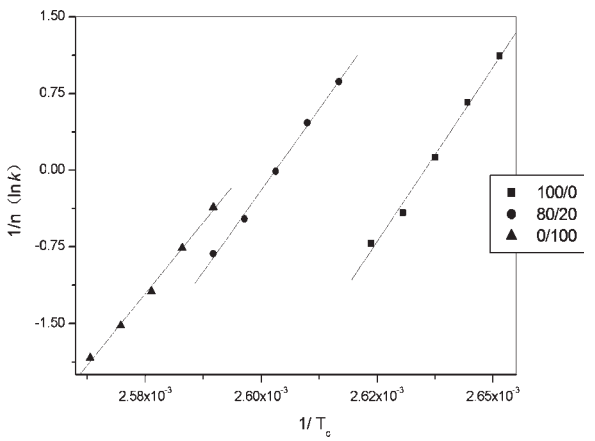

Figure 10 Arrhenius plot of $(1/n)\ln k$ versus $1/T_c$ of EPPE/mLLDPE blends for isothermal crystallization at different mLLDPE content.

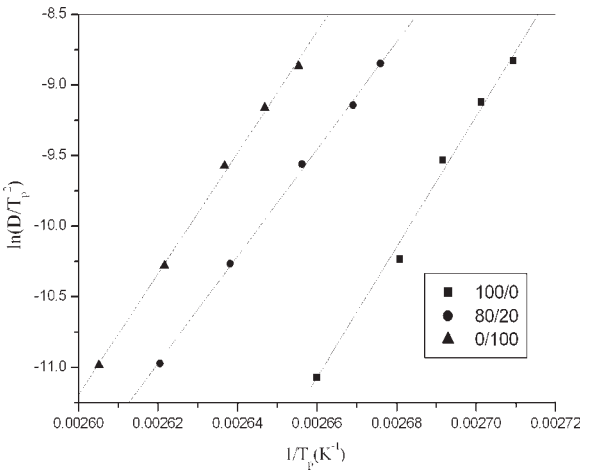

Figure 11 Kissinger plot of $\ln(D/T_p{}^2)$ versus $1/T_p$ of EPPE/mLLDPE blends for nonisothermal crystallization at different mLLDPE content.

CONCLUSIONS

The melting behaviors and crystallization kinetics of EPPE/mLLDPE were investigated with DSC. The Avrami analysis and a method developed by Mo were successful in describing the isothermal and nonisothermal crystallization process of the blends. The value of n suggested that the isothermal crystallization of the systems is heterogeneous and the growth of the crystal is not perfect. All the proofs show that the mLLDPE act as nuclei while crystallization, because the crystallization temperature of it is obviously higher than that of EPPE.

References

1. Mori, H.; Ohnishi, K.; Terano, M. Macromol Chem Phys 1998, 199, 393.
2. Xiaohua, K.; Xiaoniu, Y.; Gao, L.; Xiaoguang, Z.; Enle, Z.; Dezhu, M. Eur Polym J 2001, 37, 1855.
3. Jungang, G.; Dong, W.; Maoshang, Y.; Zihua, Y. J Appl Polym Sci 2004, 93, 1203.
4. Xikui, Z.; Tingxiu, X.; Guisheng, Y. Polymer 2006, 47, 116.
5. Lu, X. F.; Hay, J. N. Polymer 2001, 42, 9423.
6. Chaoqin, L.; Guohua, T.; Yong, Z.; Yinxi, Z. Polym Test 2002, 21, 919.
7. Herrero, C. H.; Acosta, J. L. Polymer 1994, 26, 786.
8. De Juana, R; Jauregui, A; Calahora, E; Cortazar, M. Polymer 1996, 37, 3339.
9. Lee, S. W.; Ree, M.; Park, C. E.; Jung, Y. K.; Park, C. S.; Jin, Y. S.; Bae, D. C. Polymer 1999, 40, 7137.
10. Ozawa, T. Polymer 1971, 12, 150.
11. Ozawa, T. Polymer 1978, 19, 1142.
12. Ziabicki, A. Colloid Polym Sci 1974, 6, 252.
13. Ziabicki, A. Appl Polym Symp 1967, 6, 1.

14. Liu, T. X.; Mo, Z. S.; Wang, S. E.; Zhang, H. F. Polym Eng Sci 1997, 37, 568.
15. Caze, C.; Devaux, E.; Crespy, A.; Cavrot, J. P. Polymer 1997, 38, 497.
16. Nakamura, K.; Katayama, K.; Amano, T. J Appl Polym Sci 1973, 17, 1031.
17. Chan, T. W.; Isayev, A. I. Polym Eng Sci 1994, 34, 461.
18. Avrami, M. J Chem Phys 1939, 7, 1103.
19. Avrami, M. J Chem Phys 1940, 8, 212.
20. Tobin, M. C. J Polym Sci Polym Phys Ed 1974, 12, 399.
21. Ziaee, Z.; Supaphol, P. Polymer Testing 2006, 25, 807.
22. Run, M.; Gao, J.; Li, Z. Thermochimica Acta 2005, 429, 171.
23. Yanming, D. The Practical Analyze Technology of Polymer Materials; Petro-chemical Industry Press: Beijing, China, 1997; p 293.
24. Seo, Y. S.; Kim, J. H.; Kin, K. U.; Kim, Y. C. Polymer 2000, 41, 2639.
25. Xu, W. B.; Ge, M. L.; He, P. S. J Appl Polym Sci 2001, 82, 2281.
26. Cebe, P.; Hong, S. D. Polymer 1986, 27, 1183.
27. Villanova, P. C.; Ribas, S. M.; Guzman, G. M. Polymer 1985, 26, 423.
28. Kissinger, H. E. J Res Natl Bur Stand (US) 1956, 57, 217.